# An attempt to isolate the double ridge in high multiplicity pp collisions using the transverse spherocity

Mevine Staaden

Thesis submitted for the degree of Bachelor of Science, HT17
Project Duration: 2 Months
*December 2017*


LUND
UNIVERSITY

Supervised by Peter Christiansen
Department of Physics
Division of Particle Physics
Lund University
Lund, Sweden

**Abstract**

One of the hot topics at the LHC is the double ridge observed in small systems. Originally it was found in p-Pb collisions at $\sqrt{s_{\mathrm{NN}}} = 5.02$ TeV when subtracting low multiplicity from high multiplicity events. This thesis attempts to isolate a double ridge in pp collisions at $\sqrt{s_{\mathrm{NN}}} = 13$ TeV by utilizing multiplicity and transverse spherocity. While the double ridge was not successfully isolated, the results display potential issues with the transverse spherocity selection of QGP-like events. This thesis outlines the method used for the analysis and discusses the results.

# Acknowledgements

I would like to thank Peter Christiansen for suggesting this topic to me and helping me throughout the entire process, including all the help with the theory and the coding. Furthermore I would like to thank everyone at the ALICE office for all the help and support with AliRoot and Aurora and all the encouragement throughout the past few months. A special thank you to Vytautas for helping me understand AliRoot and its different built-in functions and header files.

# Contents

# 1 Introduction

In the field of ultra-relativistic heavy-ion physics, strongly interacting matter is studied under extreme conditions such as high energy and density [1]. In the Standard Model the strong force is described with the theory of quantum chromodynamics (QCD). This theory is discussed further in Sec. 2.2, and describes the interaction between quarks and gluons [2]. QCD predicts that at high temperatures and high densities a special state called the quark-gluon plasma (QGP) exists (see Sec. 2.3). This state resembles the state of the Universe within the first microseconds after the Big Bang.

The QGP is currently studied extensively, and recent research found "Long-range angular correlations on the near and away side in p-Pb collisions at $\sqrt{s_{\mathrm{NN}}} = 5.02$ TeV" [3]. This analysis looked at two-particle correlations in high multiplicity and low multiplicity events in proton-lead (p-Pb) collisions and subtracted the latter from the first. This revealed a near-side and far-side ridge, also known as the double ridge, which supports the liquid model of the quark-gluon plasma. This ridge is attributed to "flow" (see Sec. 2.3.1) that describes the expansion of matter after the collision and has been observed to be anisotropic for heavy-ion collisions.

While many of the quark-gluon plasma theories originate in heavy-ion studies, recent research has focussed more on small systems, such as proton-proton (pp) collisions. This thesis looks at high multiplicity pp-collisions and attempts to isolate the double ridge found in the analysis mentioned previously using transverse spherocity. The theoretical and detector background will be discussed before explaining the method used in this analysis. Finally, after examining the results, there will be some discussion of the findings.

# 2 Theory

## 2.1 The Standard Model

The Standard Model describes the elementary particles: quarks, leptons and bosons, where quarks and leptons are grouped together as fermions. This can be seen in Fig. 1. The diagram shows the mass, electric charge and spin for the different particles of the standard model.

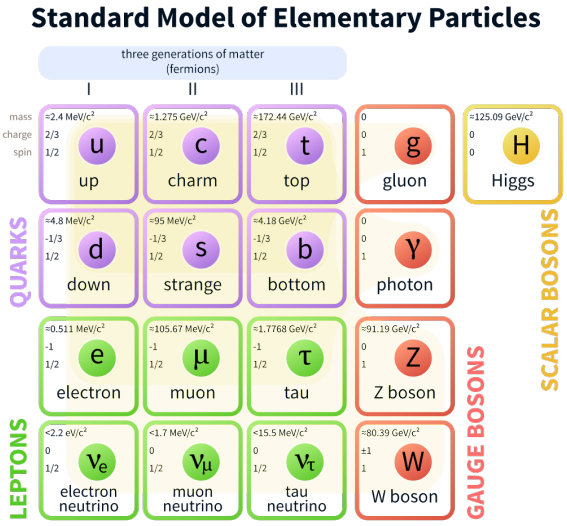


Figure 1: A diagram summarizing the Standard Model with the six quarks, six leptons, and bosons [4].

There are six types of quarks; up, down, charm, strange, top and bottom. Each of these has an anti-quark as well, that has the same mass and the opposite charge. Quarks have both electric charges and color charges. Each quark has a color charge of either red, green or blue while an anti-quark has a color charge of either anti-red, anti-green or anti-blue. This is a vital part of quantum chromodynamics and will be discussed further in the next section, Sec. 2.2. Quarks make up hadrons such as protons and neutrons.

There are six different leptons; electrons, muons and taus, plus electron neutrinos, muon neutrinos and tau neutrinos. The neutrinos have no electric charge or color charge while the other leptons have an electric charge of -1. Additionally, each of these leptons and neutrinos have anti-particles with opposite charges.

Finally, the Standard Model theorizes about forces. Bosons are the particles that allow matter particles to interact. There are four gauge bosons and one scalar boson so far. The gauge bosons are the W and Z bosons, the photon, and the gluon. The first two bosons

mediate the weak force. These two bosons have a comparably large mass and the W boson has an electric charge of +1 or -1 while the Z boson has no electric charge. The photon is the boson that mediates the electromagnetic force and has no mass or electric charge. The last gauge boson, the gluon, is responsible for strong interactions. This boson has a color charge and only interacts with quarks and other gluons. It is also massless and has no electric charge. Lastly, the scalar boson is the well-known Higgs Boson which gives particles mass.

## 2.2 Quantum Chromodynamics

Quantum chromodynamics (QCD) is the theory linked to the color charges of quarks. It can be compared to quantum electrodynamics (QED), the relativistic quantum field theory of electrodynamics. QCD has two unique properties, color confinement and asymptotic freedom.

The color confinement means that quarks cannot be observed as single quarks but instead are confined within hadrons. The color charge should be neutral (either all three colors, all three anti-colors or color–anti-color pairs), which leads to limited ways in which quarks can be observed. One of the ways in which quarks can be observed is as a combination of quarks in either baryons or mesons (together referred to as hadrons), where baryons consist of three (anti-)quarks and mesons consist of a quark and anti-quark pair. At high temperatures and high matter densities this confinement is broken. This state is called the quark-gluon plasma and is discussed further in Sec. 2.3. Comparing this to QED, where charges can be observed on a continuous spectrum, color confinement is very different and more challenging to study.

The other unique property of QCD is asymptotic freedom. Unlike QED, where the strength of the electromagnetic force becomes weaker as the distance increases, QCD observes an asymptotic behaviour for the strength of the strong force. The interactions between particles become weaker as the distance decreases. This phenomena is called asymptotic freedom as it suggests that quarks will behave as free particles for very short ranges.

## 2.3 Quark-Gluon Plasma

At high energies a phase transition occurs from hadrons to the quark-gluon plasma. This plasma occurs at high temperatures and high densities and behaves like an almost perfect liquid. In this QGP state, quarks and gluons are deconfined, which means they are no longer bound inside hadrons (baryons and mesons as discussed in Sec. 2.2) [5]. This plasma state can be achieved in high energy collisions in particle accelerators (see Sec. 3), by colliding, for example, a lead nuclei with a proton (p-Pb) or simply two lead nuclei (Pb-Pb).

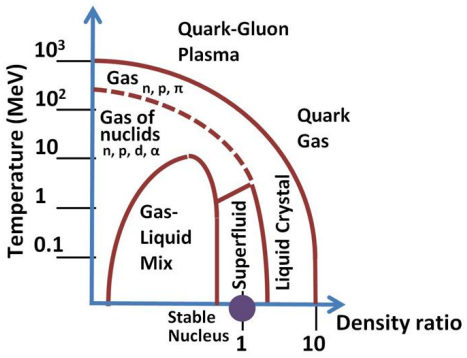


Figure 2: A diagram depicting the conditions for different states of matter [6].

The transition between the confined state and the deconfined state occurs when the energy density of the matter is in the same order as the energy density within the matter of a proton, which is at approximately 0.15 GeV/fm$^3$ [5]. Additionally, this transition occurs when the temperature $T$ is above $T_c$ (the critical temperature). The transition can be understood as a change in the degrees of freedom from hadrons to quarks and gluons. Studying the nature of this transition could help us understand the features of the quark and gluon confinement.

The quark-gluon plasma has been studied extensively at accelerators that are capable of reaching very high energies, such as the Large Hadron Collider (see Sec. 3.1) or the Relativistic Heavy Ion Collider (RHIC) [5, 7]. One analysis found that studying the QGP in proton-lead (p-Pb) collisions shows both a near side and a far side ridge [3], which was later reproduced by several other measurements. This paper will be discussed further in Sec. 2.4.

The study of the quark-gluon plasma is important for several reasons. For one, it is the primordial form of QCD matter and gives us a unique insight into the non-perturbative dynamics of quarks and gluons. This phase of matter was present during the first few microseconds of the Big Bang and astronomers think that the quark-gluon plasma could also occur in neutron stars, gamma ray bursts and supernovae due to the high baryon matter density in those objects. Finally, as mentioned previously, it could help understand the nature of the quark-gluon confinement within QCD when $T \sim T_c$ and may help provide information on the origin of baryonic mass [5].

### 2.3.1 Flow

The quark-gluon plasma (QGP) is studied in heavy ion collisions. In these collisions particles are produced and collectively boosted by a common velocity field which arises from the quick expansion of the collision system. This flow is referred to as anisotropic and results mainly from the elliptic overlap of the nuclei during the collision. This anisotropy in the particle flow can be quantified using Fourier analysis of the azimuthal distribution in relation to the systems symmetry plane angles $\Psi_n$ which are characterized by the flow coefficients $\nu_n$ [8].

$$\frac{\mathrm{d}N}{\mathrm{d}(\varphi - \Psi_n)} \propto 1 + \sum_{n=1}^{\infty} 2\nu_n \cos\left(n\left[\varphi - \Psi_n\right]\right) \tag{1}$$

Here, $\varphi$ is the azimuthal angle of the produced particle. This equation describes the anisotropic flow of the particles after heavy-ion collisions, which is a characteristic behaviour of the QGP. For elliptic flow, which is the type of flow that is important to this analysis, the flow coefficient is $\nu_2$.

## 2.4 The Double Ridge and Multiplicity

The previously mentioned paper, that found a near side and far side ridge in proton-lead (p-Pb) collisions, functioned as an inspiration for this thesis.[1] The study looked at $\Delta\eta$ and $\Delta\varphi$ and found a signal as an associated yield per trigger particle.

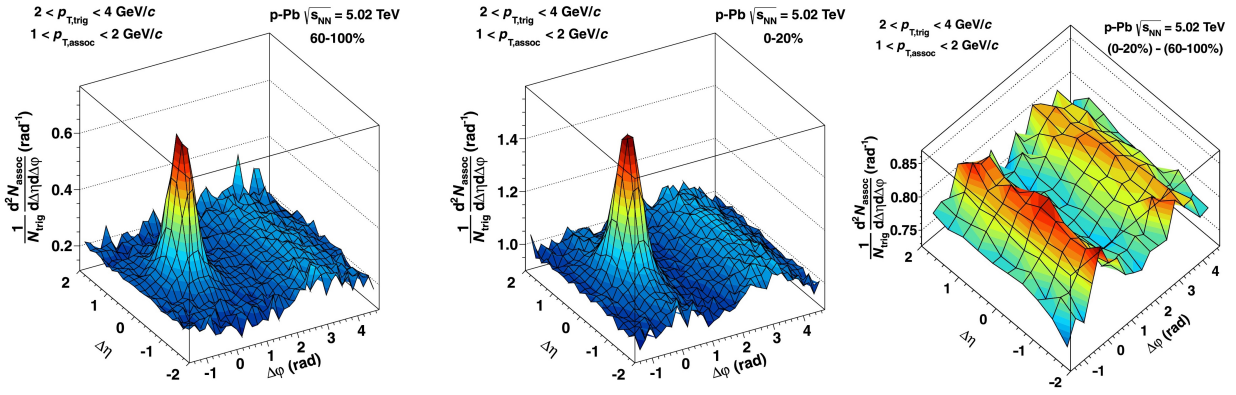


Figure 3: Results found in the Double Ridge paper [3].

[1] The near side and far side ridge will often be referred to as the double ridge throughout this paper.

The pseudorapidity, $\eta$, is the angle of the particle relative to the beam axis and is defined by

$$\eta \equiv -\ln\left[\tan\left(\frac{\theta}{2}\right)\right] \tag{2}$$

where $\theta$ is the angle between the positive direction beam axis and the momentum of the particle. In this analysis, the maximum value for $\eta$ was set to $|\eta| < 0.8$ since the double ridge paper used this limit as well and ALICE has an acceptance of $|\eta| < 0.9$ [13]. The azimuth, $\varphi$, is measured in the transverse plane (the xy-plane) and is the angle between the transverse momentum and the x-axis.

In order to get $\Delta\eta$ and $\Delta\varphi$, two-particle correlations are used in which $\eta$ and $\varphi$ values are taken from two different particles in different momentum ranges and then the difference is taken. This is discussed further in Step 1 of Sec. 4. The signal was then measured as an associated yield per trigger particle. The result then looks similar to Fig. 3, which shows a peak but also two clear ridges along $\Delta\varphi = 0$ and $\Delta\varphi = \pi$ for the entire range of $\Delta\eta$. This result can be attributed to the anisotropic flow of the particles after the collision (see Sec. 2.3.1). For two-particle correlations, the flow can be described using the following equation:

$$\frac{\mathrm{d}N_{\mathrm{pairs}}}{\mathrm{d}\Delta\varphi} \propto 1 + \sum_{n=1}^{\infty} 2\nu_{2a}\nu_{2b}\cos\left(n\Delta\varphi\right) \tag{3}$$

Here, the two different flow-coefficients $\nu_{na}$ and $\nu_{na}$ correspond to the two particles $a$ and $b$. Since this gives ${\nu_2}^2$ in two-particle correlations, the already small effect becomes much smaller. The double ridge in p-Pb collisions was found when subtracting low multiplicity events (60-100%) from high multiplicity events (0-20%).

The multiplicity is taken from the V0 Detector within the ALICE detector (see Sec. 3.2). The multiplicity of the events is given in terms of centrality, which is measured in percentiles. Multiplicities given in ranges from 0-20% thus represent a centrality of 0-20%, which corresponds to a high multiplicity. Centrality refers to "how central the event is" and is taken from summed amplitude and signal measurements from both V0 detectors, V0A and V0C (see Sec. 3.2).

## 2.5 Transverse Spherocity

The measurement of spherocity arose from $e^+e^- \to q\bar{q}$ collisions when looking at the jet axis of the quarks. Spherocity has now been adapted to hadronic collisions by looking at the spherocity in the transverse plane relative to the jets. Transverse spherocity, $S_0$, is defined by

$$S_0 \equiv \frac{\pi^2}{4}\left(\frac{\sum_i |\overrightarrow{p_{T_i}} \times \hat{n}|}{\sum_i p_{T_i}}\right)^2 \tag{4}$$

where $\hat{n}$ is the transverse unit vector that minimizes $S_0$ and $p_{T_i}$ is the transverse momentum [9]. The transverse momentum is defined by:

$$p_T \equiv \sqrt{p_x^2 + p_y^2} \tag{5}$$

The transverse spherocity can take values between 0 and 1, where smaller values correspond to more jetty events and larger values correspond to more isotropic events. Jetty events are events which have more of a back-to-back structure while isotropic events are more evenly distributed.

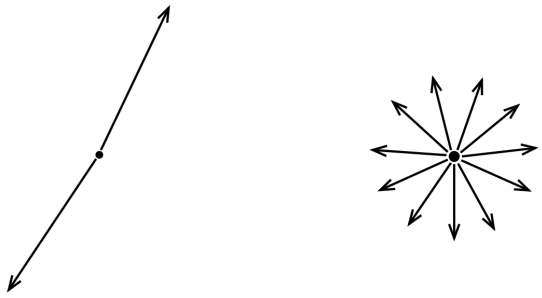

Figure 4: The extreme examples of spherocity. Events similar to the one depicted on the left are referred to as jetty events. The transverse spherocity for these events is small (close to 0). Events that are similar to the image on the right are called isotropic events. The transverse spherocity for these events has a larger value (close to 1).

# 3 Detector

The data used in this analysis is taken from the ALICE experiemnt at CERN. CERN is the European Organization for Nuclear Research that provides the experimental set up of the particle accelerator [10]. The particle accelerator used for this data was the Large Hadron Collider (LHC), discussed further in Sec. 3.1. This accelerator is equipped with several detectors such as the ATLAS [11] detector and CMS [12]. For these measurements the ALICE detector was used. While ATLAS and CMS are general purpose detectors mainly studying proton-proton (pp) collisions, ALICE stands for *A Large Ion Collider Experiment* and is optimized for heavy ion collisions. It is discussed further in Sec. 3.2.

## 3.1 Large Hadron Collider

The Large Hadron Collider (LHC) at CERN is the largest particle accelerator in the world. It is a circular accelerator, which has a circumference of 27 km and consists of superconducting magnets and an accelerating system. It utilizes the tunnel previously built for the LEP machine between 1984-1989, which was closed down in 2000 to be used for the LHC, which started collecting data in 2009. It aims to study physics beyond the Standard Model with center of mass collisions of currently up to 13 TeV in pp-collisions [13].

Its accelerating mechanism utilizes RF-cavities (radiofrequency-cavities) while the bending and focussing mechanism relies on superconducting magnets, just like many other accelerators, for example accelerators at DESY [14] or RHIC [15]. These accelerators generally used superconducting magnets that had NbTi Rutherford cables that were cooled to 4.2 K, which allows fields of 5 T or less. The magnets at the LHC also rely on Rutherford cables but are cooled to 2 K using superfluid helium, which allows the LHC to be operated at around 8 T [13].

## 3.2 ALICE

The ALICE Experiment is a detector at the LHC and is used for the study of heavy-ion collisions. It focuses on the study of quantum chromodynamics (QCD), the strong interaction part of the Standard Model (see Sec. 2.1). Its design is optimised to observe the matter at a high temperature and density, produced in nucleus-nucleus collisions.

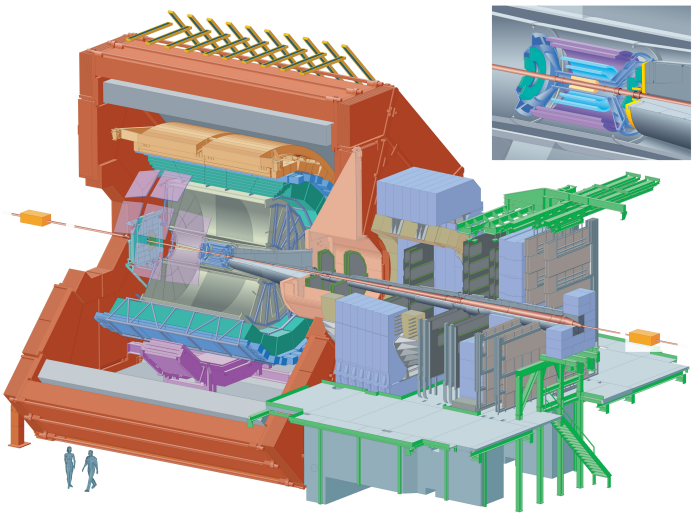

Figure 5: A schematic view of the ALICE Detector with an insert displaying the different components of the inner detector. Source: ALICE Experiment (Web) [16].

The ALICE Detector was built by a collaboration that now consists of over 1800 physicists and engineers. Its dimensions are $16 \times 16 \times 23$ m$^3$ and it weighs approximately 10 000 ton [1, 13].

The central barrel part of the detector measures hadrons, electrons, muons and photons. This central barrel part contains subdetectors, which we will look at starting from the inside and going out. It starts out with the Inner Tracking System (ITS), then the Time Projection Chamber (TPC) and then the Transition Radiation Detector (TRD) [17]. These detectors are responsible for tracking the flight and path of each electrically charged particle. The ITS and the TPC are the main detectors that track charged particles. The TPC is also capable of identifying charged particles by mesaruing the specific ionization loss [17]. Further information on the TPC can be found in Sec. 3.3.

The next set of detectors are responsible for identifying the particle. These are capable of identifying electrons, protons, kaons and pions. Among others, these detectors measure the time of flight (TOF) of each particle [1].

An important detector for our analysis is the V0 Detector, which consists of two scintillator counter arrays that are installed on either side of the interaction point [13]. It is utilized to reject beam-induced backgrounds and it also measures certain physical quantities such as the centrality of the event and particle multiplicity [18]. The multiplicity is important since it is essential to determining the centrality of nucleus-nucleus collisions. In this analysis it is used to select two different event-types, low multiplicity and high multiplicity events.

## 3.3 Time-Projection Chamber

The Time Projection Chamber (TPC) is an integral part of the ALICE detector. The research of the ALICE detector requires a robust and efficient tracking system, which is why the TPC became the main tracking system [13]. As the main tracking detector within the central barrel, it provides charged particle momentum measurements with particle identification. While the other detectors within the central barrel detectors are also used for these purposes, the TPC has been optimized for these measurements. It covers the full azimuthal angle (except for the dead zones) and has $p_T$ ranges of 0.1 GeV/c to 100 GeV/c [13].

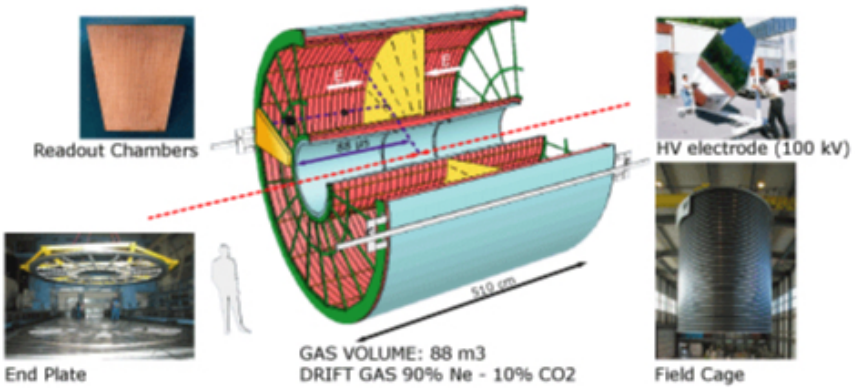


Figure 6: The layout of the Time-Projection Chamber including images of parts showing the materials used. Source: The ALICE Time Projection (TPC) (Web) [19].

The TPC is shaped like a cylinder and is filled with 90 $m^3$ of gas [17]. This gas mixture of $NeCO_2N_2$ is adapted for drift speed, low diffusion, and low radiation length [13]. This results in low multiple scattering. Additionally, the chamber is aimed to have a very minimal temperature change of $\Delta T \leq 0.1$ K within the drift volume. Since the ALICE solenoid has a temperature change of about 5 K, there are several mechanisms to keep the temperature of the TPC more or less constant. An elaborate system is required that consists of four different heat screens and two different cooling systems [13].

The next part of the TPC is the readout mechanisms. Readout chambers are placed at the two ends of the TPC and are "multi-wire proportional chambers with cathode pad readout" [13]. Since heavy ion collisions are expected to have a high track density, these chambers are designed for those situations, meaning that they have a very high granularity. In total, the TPC has over 500 000 readout channels.

# 4 Method

This analysis was done using C++ and ROOT (by CERN) [20], specifically AliRoot [21], which is a ROOT version that has several ALICE specific libraries and classes within it that simplify the analysis of tracks and events. In order to simplify the analysis further, an example code was used as a starting point and then modified further to be applied to this analysis.

## Step 1

The code was modified so that it would give us the pseudorapidity, $\eta$, and azimuth, $\varphi$, through built-in functions of AliRoot. This function took the values from analysing the tracks of the particles. In order to get the difference between two $\eta$ and $\varphi$ we needed to utilize two-particle correlations, which is a method in which one takes the $\eta$ and $\varphi$ from one particle in an event and the $\eta$ and $\varphi$ for another particle in the same event. To make this correlation work one usually uses a trigger particle in a specific $p_T$ momentum region and an associated particle from that same event within a different momentum region. Since this analysis was inspired by the recent findings of the near and far side ridge discussed in Sec. 2.3, the same values for the trigger momentum and associated momentum were used. Trigger particles had a transverse momentum in the range of $2 < p_{T_{\text{trigger}}} < 4$ GeV/c and associated particles in the range of $1 < p_{T_{\text{assoc}}} < 2$ GeV/c. The differences $\Delta\eta$ and $\Delta\varphi$ were then calculated as follows:

$$\Delta\eta = \eta_{\text{trigger}} - \eta_{\text{asocc}}$$
$$\Delta\varphi = \varphi_{\text{trigger}} - \varphi_{\text{asocc}}$$

To apply this method, the events are searched for particles within the trigger momentum range and if the event has at least one trigger particle it is searched for all the particles in the associated momentum range. Then the values for each associated particle are subtracted from the values for the trigger particle, as stated above.

These results were also normalized for the binwidth of the histograms and for the number of trigger particles.This method showed an acceptance triangle in $\Delta\eta$, shown in Fig. 7.

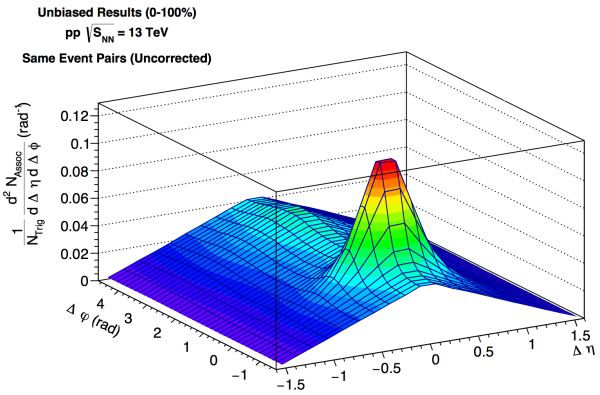


Figure 7: The uncorrected two-particle correlation function.

## Step 2

The triangle originates from the detector acceptance. To remove the triangle a method called event mixing was used. In this method, the trigger particle is taken from one event and the associated particle is taken from another event. This method only displayed the acceptance. This acceptance-triangle was then determined and normalized to have a maximum value of 1 at $\Delta\eta = 0$ and $\Delta\varphi = 0$, since theoretically and ideally there is full acceptance at $(0, 0)$. The signal values were then divided by the event-mixing values to eliminate the skewing. The event mixing results are seen in Fig. 8.

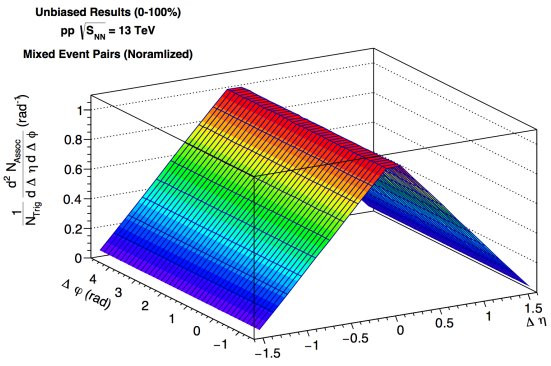


Figure 8: The acceptance triangle from event-mixing.

The original signal (Fig. 7) was divided by the normalized event mixing results (Fig. 8) to correct for the acceptance. Once this was divided we had the acceptance corrected signal

on its own. This can be seen for the unbiased analysis (0-100%) in Fig. 9. Ideally, these results should have been corrected for the efficiency of the detector to allow comparisons between different data sets. However, since this analysis only compares data from the same data set, where the efficiency is the same, this step was not necessary.

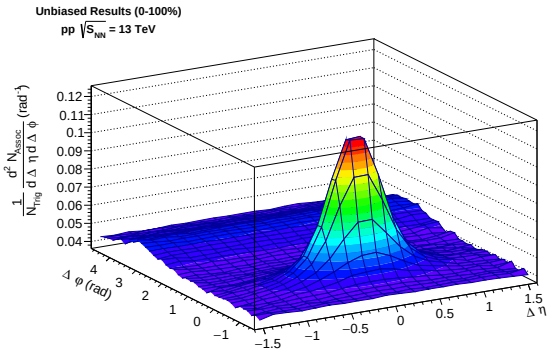


Figure 9: The acceptance-corrected two particle function.

## Step 3

The next step was to look at the different multiplicity regions and subtract the low multiplicity from the high multiplicity events. The multiplicity of the events was determined by utlizing the measurements from the V0 detector (see Sec. 3.2). The multiplicity range between 0-20% thus corresponds to 20% of events with the largest amount of energy deposited in the collision. In order to determine the ranges for low multiplicity and high multiplicity, values from the double ridge paper were used.[2] Low multiplicity events correspond to a range between 60-100% and high multiplicity events correspond to a range between 0-20% [3].

For the low multiplicity events, some noise interfered with the results when the tracks that are not from collisions were not excluded. In order to eliminate these background tracks, a track cut had to be included. This track cut analysed the tracks and determined, which belonged to events and which originated from the background.

Once the low multiplicity and high multiplicity events had been separated, the previous code could be used to do the same analysis with the two different event-types. Finally, the low multiplicity events were subtracted from the high multiplicity events to possibly obtain the double ridge. With this corrected program we managed to obtain results for both low and high multiplicities that were clear and could be worked with further. These results can be seen in the results section, Sec. 5 (Fig. 10 and 11).

[2]The double ridge paper studied p-Pb collisions while this analysis looks at pp-collisions.

## Step 4

The next step was to implement transverse spherocity, discussed more elaborately in Sec. 2.5. The following values were used to determine, which events qualified as jetty and which qualified as isotropic:

$$S_0 = \begin{cases} 0 - 0.41 & \text{jetty events} \\ 0.73 - 1 & \text{isotropic events} \end{cases} \tag{6}$$

These values were chosen because 20% of all events should be jetty and 20% should be isotropic. The values selected for the spherocity cuts were thus attained by determining between what values of spherocity the first 20% of events are located and between which values the last 20% of events lie. Using these values, we isolated the events that qualified to be jetty and which qualifed as isotropic, however, we only applied this to the high multiplicity events. To simplify, the high multiplicity events were divided into two subcategories, jetty events and isotropic events. Then the previous method was applied (steps 1-3) to these new event categories. The results can be seen in Sec. 5, Fig. 14 and 15 .

Once the signals for the different event types (low, high & jetty, and high & isotropic) were found, further analysis was done. The following subtractions were done:

- high multiplicity jetty events - low multiplicity events
- high multiplicity jetty events - high multiplicity isotropic events

The results of these subtractions are displayed in section 5 (Fig. 16 and 17) and discussed in section 6.

# 5 Results

The first results are the signals for the low and high multiplicities. These can be seen in the following graphs and display the corrected results (see section 4) for the high multiplicity events (0-20%) and the low multiplicity events (60-100%).

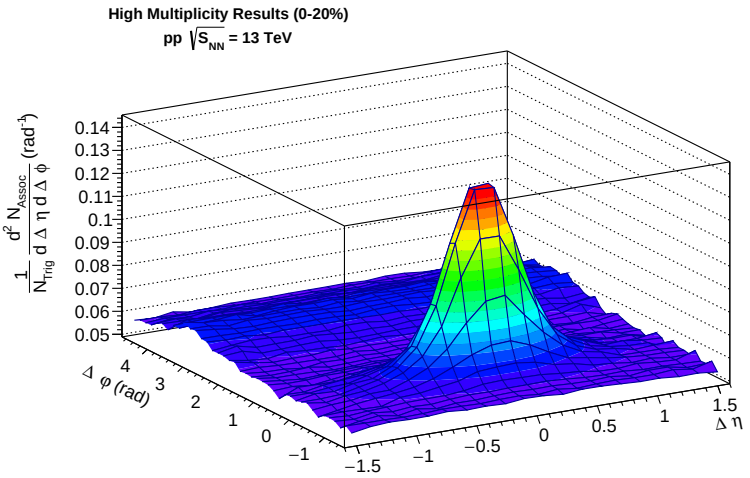


Figure 10: Corrected signal for the high multiplicity region (0-20%).

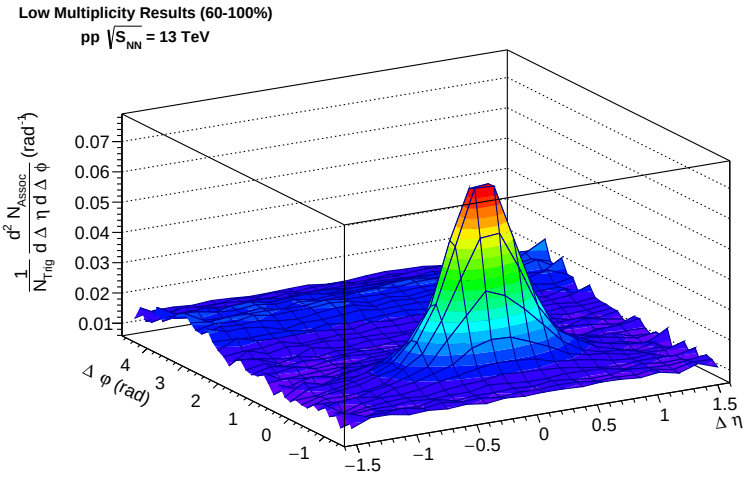


Figure 11: Corrected signal for the low multiplicity region (60-100%).

The next step was to subtract the low multiplicity events from the high multiplicity. This resulted in a fairly clear graph, however still far from the double ridge that this thesis is looking for. The results can be seen in Fig. 12.

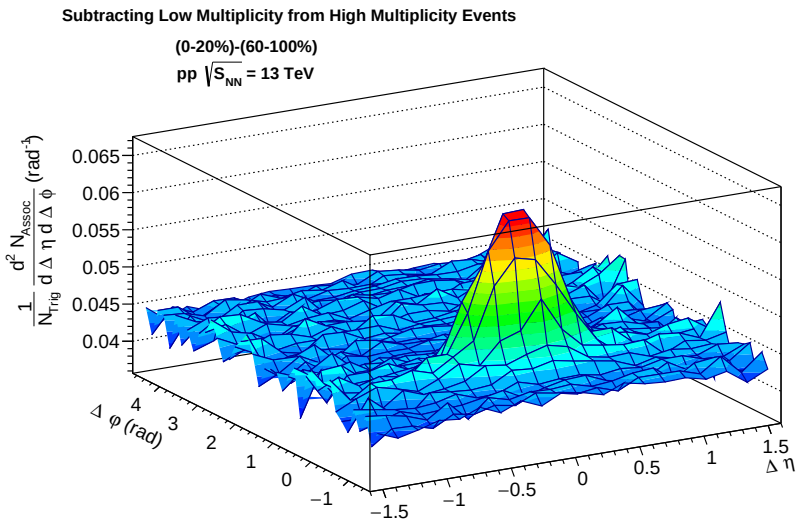


Figure 12: Signal for low multiplicity events subtracted from high multiplicity events.

An option was to look at the two-dimensional projection of the signal on $\Delta\varphi$ where the section of $\Delta\eta$ with the peak ($-0.5 < \Delta\eta < 0.5$) was removed. The signals of each bin were summed up and then normalized for the amount of bins. This result can be seen in Fig. 13.

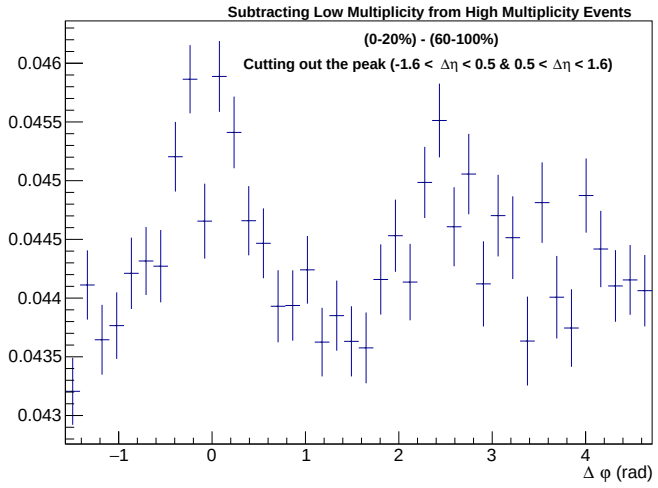


Figure 13: Projection of $\Delta\varphi$ with removed peak by removing section of $\Delta\eta$.

The next results show high multiplicity isotropic events and high multiplicity jetty events. These are discussed further in Sec. 4.

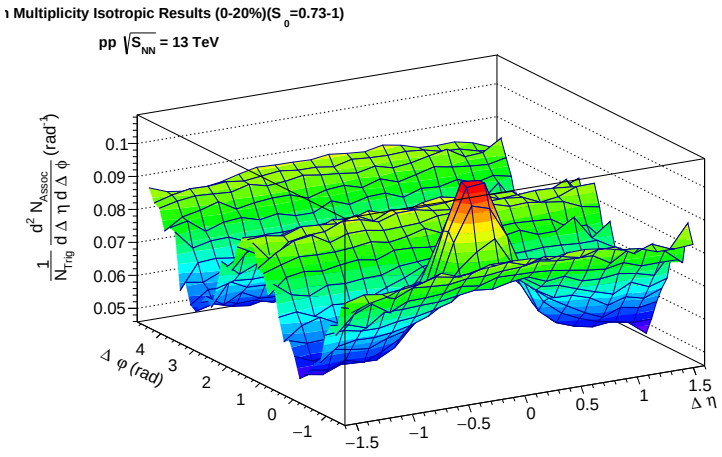


Figure 14: Corrected high multiplicity isotropic events (0-20%) with ($S_0 = 0.73 - 1$). It appears to look like an "inverted" double ridge.

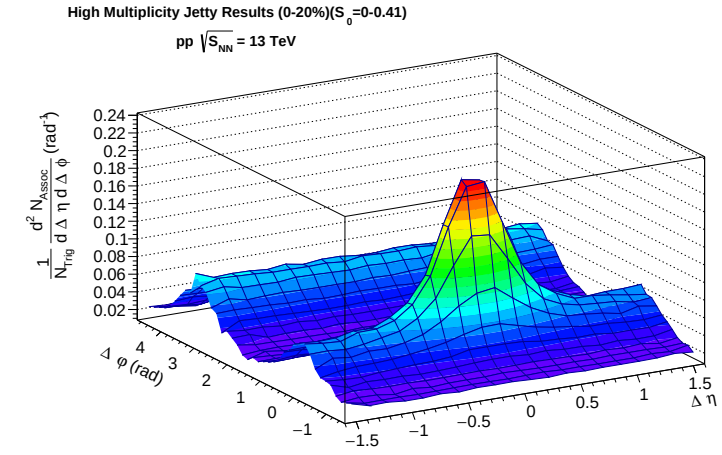


Figure 15: Corrected high multiplicity jetty events (0-20%) with ($S_0 = 0 - 0.41$).

As stated in step 4 of section 4, two subtractions were done with these results. First, low multiplicity events were subtracted from high multiplicity jetty events.

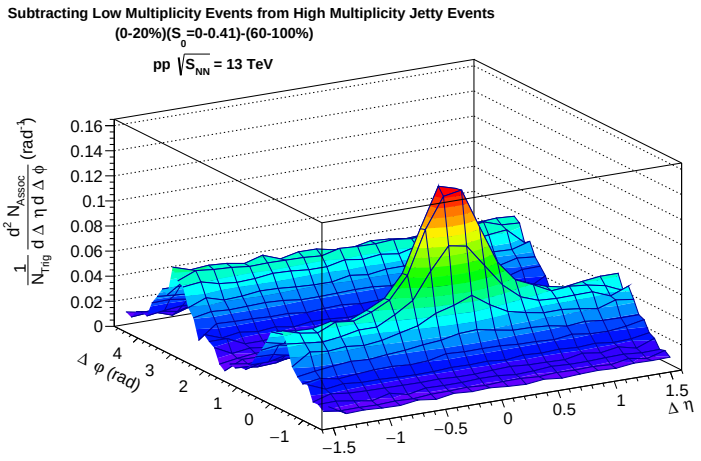


Figure 16: Low multiplicity events (60-100%) subtracted from the high multiplicity jetty events ((0-20%) and ($S_0 = 0 - 0.41$)).

Next, high multiplicity isotropic events were subtracted from high multiplicity jetty events.

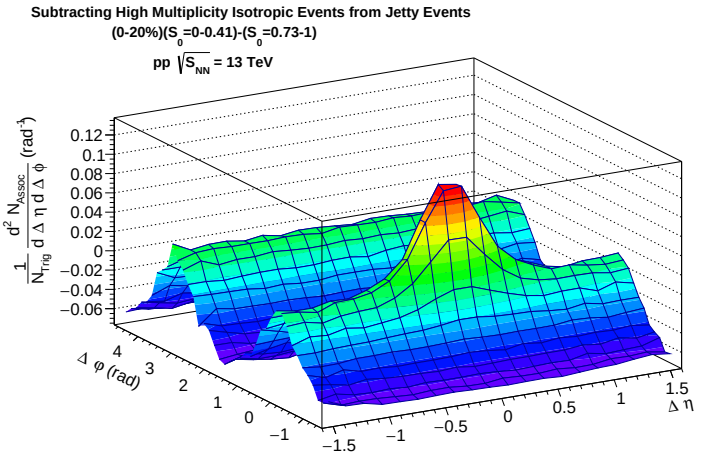


Figure 17: High multiplicity isotropic events ((0-20%) and ($S_0 = 0.73 - 1$)) subtracted from high multiplicity jetty events ((0-20%) and ($S_0 = 0 - 0.41$)).

# 6 Discussion

The results displayed in Fig. 16 and 17 look promising as both show a double ridge. While this implies that the analysis was successful and the double ridge has been found in pp-collisions, the signal for the high multiplicity isotropic events seems odd.

The "inverted" or anti-double ridge that is seen in the signal of the isotropic events (Fig. 14) is so prominent that its origin is suspicious. We think that it could be a bias from the transverse spherocity selection method. When comparing the high multiplicity jetty events (Fig. 15) to the high multiplicity isotropic events one can see how opposite they are, except for the peak. It seems that the selection of isotropic and jetty events using the spherocity gives a bias that creates the double ridge in the jetty events and thus in the subtractions (see Fig. 16 and 17).

The likely cause of this is that when selecting the isotropic events with a spherocity of $S_0 = 0.73 - 1$, high $p_T$ tracks need to be compensated with tracks at 90°. This would explain the anti-double ridge. On the other hand, the jetty events ($S_0 = 0 - 0.41$) require a back to back structure of the tracks and thus show a double ridge. Therefore, this result does not necessarily reveal anything about collectivity or the flow of the matter after proton-proton (pp) collisions, but much rather is a selection bias from our method.

We can conclude that the transverse spherocity measure is unlikely to be reliable for a correlation study since high $\nu_2$ (elliptic) flow events will be classified as jetty. This result indicates that this method has significant flaws when searching for the quark-gluon plasma (QGP) in pp collisions and a new method should be found for a better analysis.

Looking at the low and high multiplicity subtraction (figure 12), which corresponds to the method applied in the double ridge paper, we can attempt to see a double ridge. Unfortunately, the peak at $\Delta\varphi = 0$ and $\Delta\eta = 0$ is too prominent and skews the possible results too much to see the double ridge properly. The peak is a result of the two-particle correlation since this peak represents two particles that are right next to each other.

However, we can remove the peak to some extent and look at the projection of the two regions before the peak and after the peak (by removing the region $-0.5 < \Delta\eta < 0.5$). While the double ridge is not as smooth as anticipated, a double ridge can be seen faintly. However, this method summed up all the values in the selected $\Delta\eta$ regions, but this does not reveal whether it is actually a ridge at a constant level or whether it is several bumps that add up to the result. With more data and an improved method the double ridge may be even clearer. This should be studied further since finding a double ridge in small systems may be indicative of the QGP forming in small-systems or might invalidate the double ridge as an observable that indicates the QGP in heavy-ion collisions.

Therefore, the attempt in finding the double ridge in pp-collisions using transverse sphericity was technically successful in jetty events, but biased in its selection and therefore is regarded as not successful. The attempt to find it using low and high multiplicities was merely indicative of a double ridge but not fully successful.

# 7 Outlook

Further research in the fields of small systems in relation to ultra-relativistic heavy ion physics should be done to determine a better way to isolate QGP-like events in small systems. Additionally, the results suggest that there is a possibility to find the double ridge using the subtraction of low-multiplicity from high-multiplicity events if the peak is removed more thoroughly. Therefore, further research could attempt to find a method that successfully removes the peak fully to possibly find a clearer double ridge. Finding these QGP-like events in pp-collisions would be helpful in understanding the nature of the deconfinement and the transitions between confined and deconfined matter further.

# References


[1] J. Schukraft [ALICE Collaboration], "Heavy Ion physics with the ALICE experiment at the CERN LHC", Phil. Trans. Roy. Soc. Lond. A **370** (2012) 917 doi:10.1098/rsta.2011.0469 [arXiv:1109.4291 [hep-ex]].

[2] Columbia Electronic Encyclopedia, 6th Edition, COlumbia University Press 2017, "Quantum Chromodynamics" `http://ludwig.lub.lu.se/login?url=http://search.ebscohost.com.ludwig.lub.lu.se/login.aspx?direct=true&db=lfh&AN=39027218&site=eds-live&scope=site`,

[3] B. B. Abelev *et al.* [ALICE Collaboration], "Long-range angular correlations on the near and away side in $p$-Pb collisions at $\sqrt{s_{NN}} = 5.02$ TeV" Phys. Lett. B **719** (2013) 29 doi:10.1016/j.physletb.2013.01.012 [arXiv:1212.2001 [nucl-ex]].

[4] Fehling, Dave. The Standard Model of Particle Physics: A Lunchbox's Guide. The Johns Hopkins University. Retrieved on 2008-12-03. License: `https://creativecommons.org/licenses/by/3.0/deed.en`

[5] M. Gyulassy and L. McLerran, "New forms of QCD matter discovered at RHIC", Nucl. Phys. A **750** (2005) 30 doi:10.1016/j.nuclphysa.2004.10.034 [nucl-th/0405013].

[6] Brews O'Hare, "Phase Diagram of Nuclear Matter patterned after 'Elements of Nuclei' by Phillip John Seimens, Aksel S. Jensen." License: `https://creativecommons.org/licenses/by-sa/3.0/`

[7] X. Zhu [ALICE Collaboration], "Two-particle correlations in pp and Pb-Pb collisions with ALICE", arXiv:1311.2394 [hep-ex].

[8] R. A. Bertens [ALICE Collaboration], "Anisotropic flow of inclusive and identified particles in PbPb collisions at $\sqrt{s_{NN}} = 5.02$ TeV with ALICE", Nucl. Phys. A **967** (2017) 385. doi:10.1016/j.nuclphysa.2017.04.025

[9] A. Önnerstad, "Separation of Hard and Soft Production in High Multiplicity pp Collisions using Transverse Spherocity", Bachelor Thesis, Lund University, Lund, Sweden, December 2016.

[10] CERN - About. Url: `http://home.cern/about`

[11] CERN - ATLAS. Url: `https://home.cern/about/experiments/atlas`

[12] CERN - CMS. Url: `https://home.cern/about/experiments/cms`

[13] R. Voss and A. Breskin, "The CERN Large Hadron Collider, accelerator and experiments,"

[14] DESY - Home. Url: http://www.desy.de/index_eng.html

[15] RHIC - Home. Url: https://www.bnl.gov/rhic/default.asp

[16] ALICE Collaboration - The ALICE Experiment (2008). Url: http://aliceinfo.cern.ch/Public/en/Chapter2/Chap2Experiment-en.html

[17] B. Abelev *et al.* [ALICE Collaboration], "Performance of the ALICE Experiment at the CERN LHC," Int. J. Mod. Phys. A **29** (2014) 1430044 doi:10.1142/S0217751X14300440 [arXiv:1402.4476 [nucl-ex]].

[18] E. Abbas *et al.* [ALICE Collaboration], "Performance of the ALICE VZERO system", JINST **8** (2013) P10016 doi:10.1088/1748-0221/8/10/P10016 [arXiv:1306.3130 [nucl-ex]].

[19] ALICE Collaboration - The ALICE Time Projection Chamber (TPC) (2008). Url: http://aliceinfo.cern.ch/Public/en/Chapter2/Chap2_TPC.html

[20] ROOT Data Analysis Framework. Url: https://root.cern.ch

[21] ALICE - Offline. Url: http://alice-offline.web.cern.ch